7.3. Thermal neutron detection

BY P. CONVERT AND P. CHIEUX

7.3.1. Introduction

In this chapter, we shall be concerned with the detection of neutrons having thermal and epithermal energies in the range 0.0002–10 eV (20–0.1 Å). Given the cost and the rarity of the neutron sources, it is clear that the recent trends in neutron diffractometry are more and more in the direction of designing new instruments around highly efficient and complex detection systems. These detection systems become more and more adapted to the particular requirements of the different experimental needs (counting rate, size, resolution, definition, shielding and background, TOF, *etc*.). It is therefore difficult to speak about neutron detectors and intensity measurements as such without reference to the complete spectrometers, and this should include the on-line computer.

Most neutron detectors for research experiments have been created and developed using fission reactors as neutron sources [*i.e.* with an upper limit of usable energy of 0.5 eV (0.4 Å)]. Given the relatively low intensity of reactor neutron beams, a very successful effort has been made to increase the detector efficiency and the detection area as much as possible. The recent construction of pulsed neutron sources extends the range of incident energy to at least 10 eV and generalizes the use of time-of-flight (TOF) techniques. A broad range of fully operational neutron detectors, well adapted to reactors as neutron sources, is commercially available, but this is not yet the case for pulsed sources. Probably due to the variation of intensity of the early neutron beams, it is a tradition in neutron research to monitor the incident flux with a low-efficiency detector, which in the best case has a stability of the order of 10^{-3}, *i.e.* sufficient for most experiments.

7.3.2. Neutron capture

Neutrons' lack of charge and the fact that they are only weakly absorbed by most materials require specific nuclear reactions to capture them and convert them into detectable secondary particles. Table 7.3.2.1 lists the neutron-capture reactions that are commonly used in thermal neutron detection. The incoming thermal neutron brings a negligible energy to the nuclear reaction, and the secondary charged particles or fission fragments are emitted in random directions following the conservation-of-momentum law $\sum m_i v_i = 0$. The capture or absorption cross sections for a number of nuclei of interest are plotted as a function of neutron energy in Fig. 7.3.2.1. These cross sections are commonly expressed in barns (1 barn = 10^{-28} m^2). At low energies, they are inversely proportional to neutron velocity, except in the case of Gd, which has a nuclear resonance at 0.031 eV. The total efficiency ε of neutron detection can be expressed by the equation

$$\varepsilon = \xi[1 - \exp(-N\sigma_a t)], \qquad (7.3.2.1)$$

where N is the number of absorbing nuclei per unit volume, σ_a is their energy-dependent absorption cross section, and t is the thickness of the absorbing material. The factor $1 - \exp(-N\sigma_a t)$ gives the neutron-capture efficiency, while ξ is a factor ≤ 1 that depends on the detector geometry and materials (absorption and scattering in the front window) and on the efficiency of the secondary particles.

7.3.3. Neutron detection processes

A detection process consists of a chain of events that begins with the neutron capture and ends with the macroscopic 'visualization' of the neutron by a sensor (electronic or film). The quality of a detection process will depend on the efficiency of the conversion steps and on the characteristics of the emission steps, which alternate in the process (see Table 7.3.3.1). We present below typical detection processes.

7.3.3.1. *Detection via gas converter and gas ionization: the gas detector*

The neutron capture and the trajectories of the secondary charged particles as well as the specific gas ionization along these trajectories are presented in Figs. 7.3.3.1(*a*) and (*b*). Since the gas ionization energy is about 30 eV per electron (42 eV for ^{3}He and 30 eV for CH_4), there are about 25 000 ion pairs (e^-, He^+ or e^-, CH_4^+) per captured neutron. Gases such as CH_4 or C_3H_8 are added to diminish the length of the trajectories, *i.e.* the wall effect [see Subsection 7.3.4.2(*b*)].

We give in Fig. 7.3.3.1(*c*) the proton range of an ^{3}He neutron-capture reaction in various gases (Fischer, Radeka, & Boie, 1983). A schematic drawing of a gas monodetector, which might be mounted either in axial or in radial orientation in the neutron beam, is given in Fig. 7.3.3.1(*d*).

For this type of detector, the efficiency as a function of the gas pressure, or gas-detector law, is written as

$$\varepsilon(\lambda) = \xi[1 - \exp(-bPt\lambda)],$$

with P (atm) = the detector-gas pressure at 293 K, t (cm) = the gas thickness, and λ (Å) = the detected neutron wavelength. The numerical coefficient b, obtained at 293 K from the ideal gas law, the Avogadro number N_A, and the gas absorption cross section σ_a (barns) at $\lambda_0 = 1.8$ Å, is

$$b = \frac{273}{293} \times \frac{N_A}{22\,414} \times \frac{\sigma_a}{\lambda_0}.$$

For ^{3}He, with $\sigma_a = 5333$ barns at $\lambda_0 = 1.8$ Å, $b = 0.07417$; for $^{10}BF_3$, with $\sigma_a = 3837$ barns at $\lambda_0 = 1.8$ Å, $b = 0.0533$. We give in Table 7.3.3.2 a few examples of gas-detector characteristics.

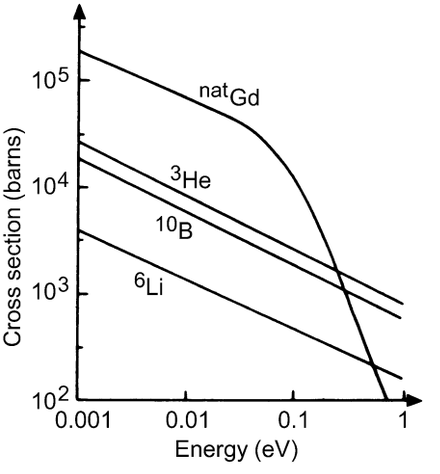

Fig. 7.3.2.1. The capture cross sections for a number of nuclei used in neutron detection. [Adapted from Convert & Forsyth (1983).]

Table 7.3.2.1. *Neutron capture reactions used in neutron detection*

n = neutron, p = H^+ = proton, t = $^3H^-$ = triton, $\alpha = {}^4H^+$ = alpha, e^- = electron

Capture reaction	Cross section at 1 Å (barns)	Secondary-particle energies (MeV)
$^3He + n \rightarrow t + p$	3000	t 0.20 p 0.57
$^6Li + n \rightarrow t + \alpha$	520	t 3.74 α 2.05
$^{10}B + n \rightarrow {}^7Li^* + \alpha$ (93%) $\hookrightarrow {}^7Li + \gamma$ $\rightarrow {}^7Li + \alpha$ (7%)	2100	α 1.47 ^7Li 0.83 γ 0.48 α 1.78 ^7Li 1.01
$^{157}Gd + n \rightarrow Gd^*$ $\hookrightarrow \gamma$ + conversion electrons	74000 (^{nat}Gd: 17000)	e^- spectrum 0.07 to 0.182 γ spectrum up to 8
$^{235}U + n \rightarrow$ fission fragments	320	Fission fragments up to 80

There are two modes of operation.

In the case of *direct collection of charges*, the 25 000 electrons corresponding to one neutron capture (*primary electrons*) are collected by the anode in about 100–500 ns, and generate an input pulse in the charge preamplifier (see Section 7.3.4).

If the electrical field created by the high voltage applied to the anode exceeds a critical value, the electrons will be accelerated sufficiently to produce a cascade of ionizing collisions with the neutral molecules they encounter, the new electrons liberated in the process being called *secondary electrons*. This phenomenon, *gas multiplication*, occurs in the vicinity of the thin wire anode, since the field varies as $1/r$. The avalanche stops when all the free electrons have been collected at the anode. With proper design, the number of secondary electrons is proportional to the number of primary electrons. For cylindrical geometries, the multiplication coefficient M can be calculated (Wolf, 1974). This type of detection mode is called the proportional mode. It is very commonly used because it gives a better signal-to-noise ratio (see Section 7.3.4).

A few critical remarks about gas detectors:

(i) Some gases have a tendency to form negative ions by the attachment of a free electron to a neutral gas molecule, giving a loss of detector current. This effect is negligible for ^3He but it limits the use of $^{10}BF_3$ to about 2 atmospheres pressure, although traces of gases such as O_2 or H_2O (*e.g.* detector materials and wall outgasing) are often the reason for loss by attachment.

(ii) Pure ^3He and $^{10}BF_3$ gas detectors are practically insensitive to γ radiation. This is no longer the case when additional gases, which are necessary for ^3He, are used, although the polyatomic additives C_3H_8 and CF_4 are much better than the rare gases Kr, Xe, and Ar (Fischer, Radeka & Boie, 1983).

(iii) For various reasons (the price of ^3He and $^{10}BF_3$ and the toxicity of BF_3), neutron gas detectors are closed chambers, which must be leak-proof and insensitive to BF_3 corrosion. The wall thickness must be adapted to the inside pressure, which sometimes implies a rather thick front aluminium window (*e.g.* a 10 mm window for a 16 bar ^3He gas position-sensitive detector; aluminium is chosen for its very good transmission of neutrons, about 90% for 10 mm thickness).

7.3.3.2. *Detection via solid converter and gas ionization: the foil detector*

This mode of detection is generally used for monitors. In a typical design, a ^{10}B deposit of controlled thickness, for example $t = 0.04\,\mu m$ giving a capture efficiency of 10^{-3} at $\lambda = 1$ Å, is made on a thin aluminium plate (see Fig. 7.3.3.2). One of the two particles (α, Li) produced in the solid by the capture reaction is absorbed by the plate; the other escapes and ionizes the gas. The electrons produced are collected by the aluminium plate, itself acting as the anode, or by a separate anode wire, allowing the use of the proportional mode. The detection efficiency is proportional to the deposit thickness t, but t must be kept less than the average range r of the secondary particles in the deposit (for ^{10}B, $r_\alpha = 3.8\,\mu m$ and $r_{Li} = 1.7\,\mu m$), which limits the efficiency to a maximum value of 3–4% for $\lambda = 1$ Å. The fraction of the secondary particle energy that is lost in the deposit reduces the detector current, *i.e.* the signal-to-noise ratio, and worsens the amplitude spectrum (see Section 7.3.4).

7.3.3.3. *Detection via scintillation*

In the detection process *via* scintillation (see Table 7.3.3.1), the secondary particles produced by the neutron capture ionize and excite a number of valence-band electrons of the solid scintillator to high-energy states, from which they tend to decay with the emission of a light flash of photons detected by a photomultiplier [see Fig. 7.3.3.3(*a*)]. A number of conditions must be satisfied:

(i) The scintillation must be immediate after the neutron-capture triggering event.

(ii) The scintillation decay time must be short. It depends on materials, and is around 50–100 ns for lithium silicate glasses.

(iii) A large fraction of the energy must be converted into light (rather than heat).

(iv) The material must be transparent to its own radiation.

Most thermal neutron scintillation detectors are currently based on inorganic salt crystals or glasses doped with traces of an activating element (Eu, Ce, Ag, *etc.*) (extrinsic scintillators). (A plastic scintillator might be considered to be a solid organic solution with a neutron converter.)

The use of extrinsic scintillators (Convert & Forsyth, 1983), although less efficient energetically, permits better decoupling of the energy of the photon-emitting transition (occurring now in the activator centres) from that of the valence-band electron excitation or ionization energy. The crystal or glass is then transparent to its own emission, and the light emitted is shifted to a wavelength better adapted to the following optical treatment.

Table 7.3.3.1. *Commonly used detection processes*

	1st conversion (neutron captures)	2nd conversion	3rd conversion	Sensor
	Capture/solid $\rightarrow e^-$ $n + {}^{157}Gd$			Film
Gas ionization	Capture/gas $n + {}^3He \rightarrow p + t$	Gas ionization $\rightarrow e^-$ (^3He + add. gas)		Electronics
	Capture/solid $n + {}^{10}B, {}^6Li, {}^{235}U$ fission products	Gas ionization $\rightarrow e^-$ (*e.g.* Ar + CO_2)		Electronics
Scintillation	Capture/solid:	Fluorescence/solid:		
	LiF + ZnS(Ag) $n + {}^6Li \rightarrow \alpha + t$	LiF + ZnS(Ag) $\rightarrow \nu$		Film
	LiF + ZnS(Ag) $n + {}^6Li \rightarrow \alpha + t$	LiF + ZnS(Ag) $\rightarrow \nu$	Photoelectric effect $\rightarrow e^-$	Electronics
	Ce^{3+} enriched Li glass $n + {}^6Li \rightarrow \alpha + t$	Ce^{3+} enriched Li glass $\rightarrow \nu$	Photoelectric effect $\rightarrow e^-$	Electronics

ν = photon.

Table 7.3.3.2. *A few examples of gas-detector characteristics*

Detection gas	Additional gas	Gas pressure (atm)	Useful detection volume (mm × mm)	Mounting	Capture efficiency	
					$\lambda = 1$ Å	$\lambda = 2$ Å
$^{10}BF_3$		1	$L = 200$, Ø = 50	Axial Radial*	65.5% 23.4%	88.1% 41.3%
^3He		5	$L = 100$, Ø = 50	Axial Radial*	97.5% 84.4%	99.9% 97.5%
^3He		8	$L = 250$, Ø = 10	Radial*	44.7%	69.5%
^3He (monitor)	C_3H_8	2	100 × 40 × 40		10^{-5} to 10^{-3}	

* Value calculated for the diameter.

In order to maximize the light collected by the photomultiplier [Fig. 7.3.3.3(*b*)], a light reflector is added in front of the scintillator, and a light coupler adapts the dimensions of the scintillator to that of the photomultiplier (PM). The area of the scintillator might be very large (up to 1 m^2). The optimum thickness of a glass scintillator is about 1 to 2 mm, corresponding to a neutron detection efficiency of 40 to 97% for $\lambda = 1.8$ Å, depending on the ^6Li concentration (Strauss, Brenner, Chou, Schultz & Roche, 1983). In a Ce-doped Li silicate glass, the number of photons emitted per captured neutron is about 9000, giving finally about 1500 electrons at the photocathode in the optimum light-coupling configuration. The number of photons emitted per captured neutron, the number of those reaching the photocathode, and the scintillator decay time are parameters that might differ by an order of magnitude, depending on the scintillator material. However, the glass scintillator remains for the time being the best choice, since the possible gains given by other materials, in decay time or in the number of photons emitted, are always very severely offset by poor light output (*e.g.* the plastic scintillator). It is very important to maximize the number of photons per neutron reaching the photocathode, since this will help to discriminate between neutrons and γ rays [see Fig. 7.3.4.2(*e*)]. The optical coupling between the different parts of the detection system must be of very good quality.

7.3.3.4. *Films*

Films are classed as position-sensitive detectors. Two types of neutron converter are used in neutron film-detection processes. In the case of the scintillation film system, a light-sensitive film is pressed close to one or between two plastic $^6LiF/ZnS(Ag)$ scintillator screens (Thomas, 1972). In the case of the Gd-foil

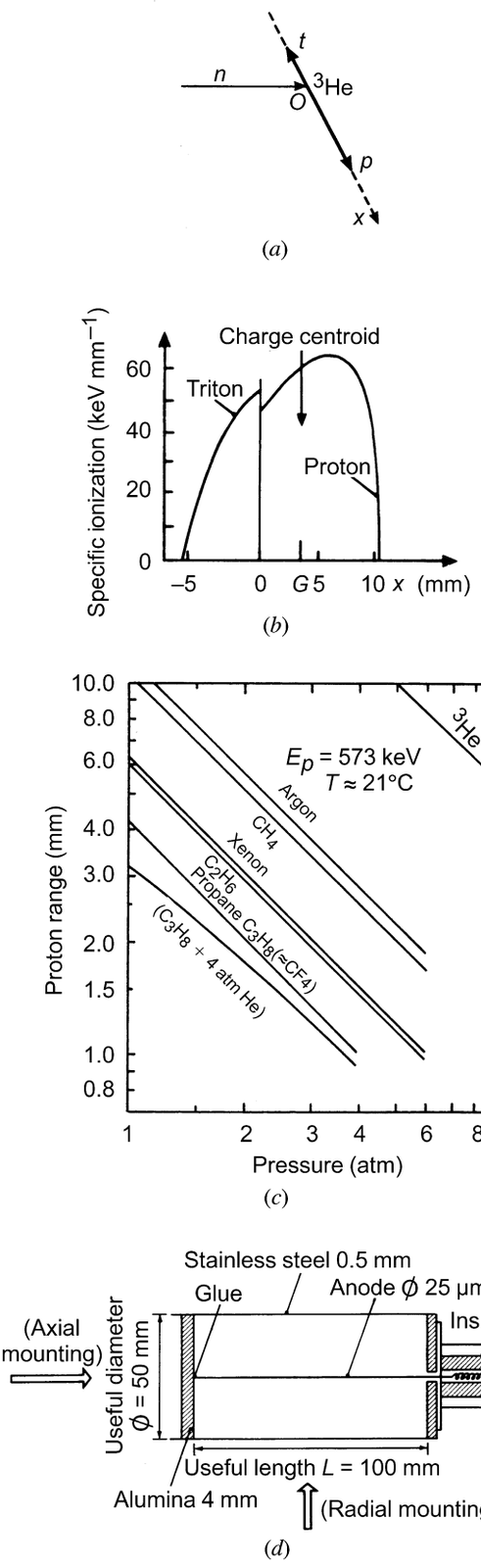

Fig. 7.3.3.1. (*a*) Neutron capture by an ^{3}He atom and random-direction trajectory (*Ox*) of the secondary charged particles in the gas mixture. (*b*) Calculated specific ionization along the proton and triton trajectory in a 65% ^{3}He/35% CH_4 mixture at 300 K and atmospheric pressure (Whaling, 1958). [Reproduced from Convert & Forsyth (1983).] (*c*) Range of a 0.57 MeV proton (from ^{3}He neutron capture) as a function of the pressure of various gases. [Reproduced from Convert & Forsyth (1983).] (*d*) Schematic drawing of a gas monodetector. The arrows represent the incoming beam.

converter, the conversion electrons are emitted isotropically, with a main energy peak at 72 keV, and collected by an X-ray film in close contact with the converter (Baruchel, Malgrange & Schlenker, 1983).

In addition to the advantages given by the film technique in itself (simplicity, low price, direct picture, *etc.*), neutron photographic methods give the best spatial resolution. However, the resolution is inversely related to the detector efficiency and thickness. A good compromise appears to be a thickness of 0.25 mm for a plastic scintillator [*i.e.* a capture efficiency of about 12% and a resolution of 0.1 mm for a one-screen converter at $\lambda = 1$ Å; see the size of the ionization volumes in a scintillator, Fig. 7.3.3.3(*a*)]. Here, however, as in light scattering, the optical density depends on the exposure time as well as on the incoming flux (Schwartzschild effect), which necessitates a calibration (Hohlwein, 1983). For a natural Gd-foil converter, an optimum thickness is 0.025 mm, giving a resolution of 0.020 mm. The Gd-foil film detector is one order of magnitude

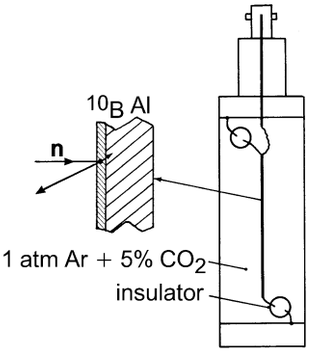

Fig. 7.3.3.2. Typical design of a ^{10}B-foil detector.

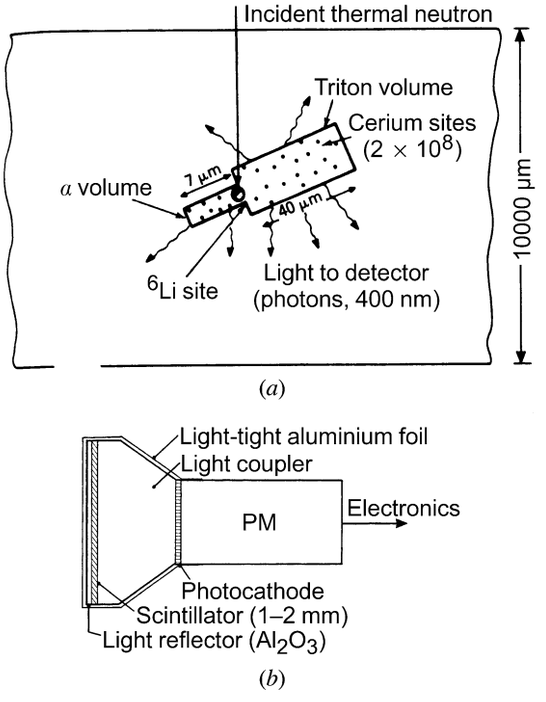

Fig. 7.3.3.3. (*a*) Schematic representation of the neutron capture, secondary α, and triton ionization volumes, and scintillator light emission in a cerium-doped lithium silicate glass. [Reproduced from Convert & Forsyth (1983).] (*b*) Schematic representation of a scintillation detector.

less efficient than the scintillator, but, as in electron microscopy, the optical density is nearly proportional to the exposure. This explains the use of the Gd foil in neutron-diffraction topography.

If we take into account the possible inhomogeneity of the converter and the difficulties related to the film (homogeneity, development, and photodensitometry), an accuracy of 5 to 10% is achievable in the intensity measurements under good conditions.

Owing to the differences in the processes, neutron photographic techniques are much more efficient than those for X-rays. In the case of the plastic scintillator, the gain is about 10^3, which compensates for the much lower neutron fluxes.

7.3.4. Electronic aspects of neutron detection

7.3.4.1. *The electronic chain*

Each collected burst of electrons, corresponding to one captured neutron, will be successively amplified, identified (discriminated), and transformed to a well defined signal, by a chain of electronic devices that are represented in Fig. 7.3.4.1. In the case of the gas detector, the complete electronic chain is generally contained in a grounded metallic box acting as an electrical shield. The detector is connected to this box *via* a coaxial cable as short as possible to avoid noise and parasitic capacitance. A high-voltage power supply feeds the detector anode through a filter. The charge-sensitive preamplifier contains a field-effect transistor (FET) to minimize the background noise, since, from the detector up to this stage, the electronic level is very low. At the output of the FET, the pulse corresponding to one neutron has an amplitude of about 20 mV. This pulse enters an operational amplifier with adjustable gain G, which delivers a signal of about 2 V, the analogue signal (ANA). The electronic pulse-rise time (0.5 to a few μs) is adapted to the detector electron-collecting time, *i.e.* its amplitude is roughly proportional to the number of electrons collected at the anode. The last part of the electronic chain is a discriminator with an adjustable threshold, followed by a trigger delivering a calibrated signal (*e.g.* +5/0 V), called the logic signal (LOG), which is sent to a scaler.

In the case of the scintillator, the photomultiplier ensures the conversion of light to electrons and produces a strongly amplified electronic signal that is processed through a discriminator and trigger as for the gas detector.

7.3.4.2. *Controls and adjustments of the electronics*

For the gas detector, there are basically three parameters to be adjusted, the gas-amplification coefficient M (a function of the detector high voltage), the electronic amplification gain G, and the discriminator threshold T. Since these adjustments are interactive, the high voltage is initially set at the value given by the manufacturer. The gain G is adjusted in order not to saturate the amplifier. When the electronic amplifier power supply voltage is 5 V, a typical setting of the pulse maximum amplitudes is about 3 V.

We present now the three types of operation necessary to adjust the electronics.

(*a*) *Control of the pulse shape*. The analogue pulse ANA (see Fig. 7.3.4.1) is directly observed with an oscilloscope. Depending on the construction of the electronic chain, it is important to verify if the input of the oscilloscope (or of the multichannel analyser, see below) must be adapted with a 50 Ω impedance or not. This will ensure that the amplitude of the analogue pulse and the accessible value of the voltage threshold are on the same scale (and not different by a factor of two). Fig. 7.3.4.2(*a*) shows characteristic shapes obtained when triggering the oscilloscope at, say, 0.2 V and observing a $^{10}BF_3$ gas detector either pulse by pulse or in a continuous way. This type of display allows the trained user to check the noise level, the amplitudes of the neutron pulses, the quality of the pulse shape, and the presence of any anomalous signal such as one due to flashes of parasitic electronic or electric noise (*e.g.* 50 Hz). γ rays produce fewer electrons than neutrons, so that the corresponding pulses are of a lower amplitude (by a factor of 1/5 to 1/20).

(*b*) *Control of the distribution of the pulse amplitudes*. The distribution of amplitudes of the various pulses in number of pulses per amplitude increment dN/dA is analysed and displayed using a multichannel analyser. Fig. 7.3.4.2(*b*) shows the amplitude spectrum for a $^{10}BF_3$ gas detector. The main peak at A_0 corresponds to the main neutron-capture reaction (2.3 MeV, 93%). From its FWHM, we define the detector electronic resolution $\Delta A/A_0$. The right-hand-side small peak is due to the 2.8 MeV, 7% capture reaction. The tail of amplitudes down to $4A_0/11$ corresponds to neutrons captured near the detector walls, which stop some of the secondary-particle trajectories (wall effect). The existence of a deep valley [see Fig. 7.3.4.2(*b*)] where the discriminator threshold T is placed ensures that all captured neutrons, and nothing else, are counted. The width of this valley guarantees good detection stability. Three effects might reduce this valley. Worsening of the gas quality will reduce all the pulse amplitudes (neutron and gamma), an increase in electronic noise will result in a resolution loss affecting the valley on both sides, and a high level of γ radiation will produce a pile up of the independent γ pulses, increasing their amplitude.

(*c*) *Optimization of the threshold and high-voltage values*. In order to set the threshold T at its optimum value for discrimination and stability, the total number of counts in the detector per unit time is plotted as a function of the threshold, for

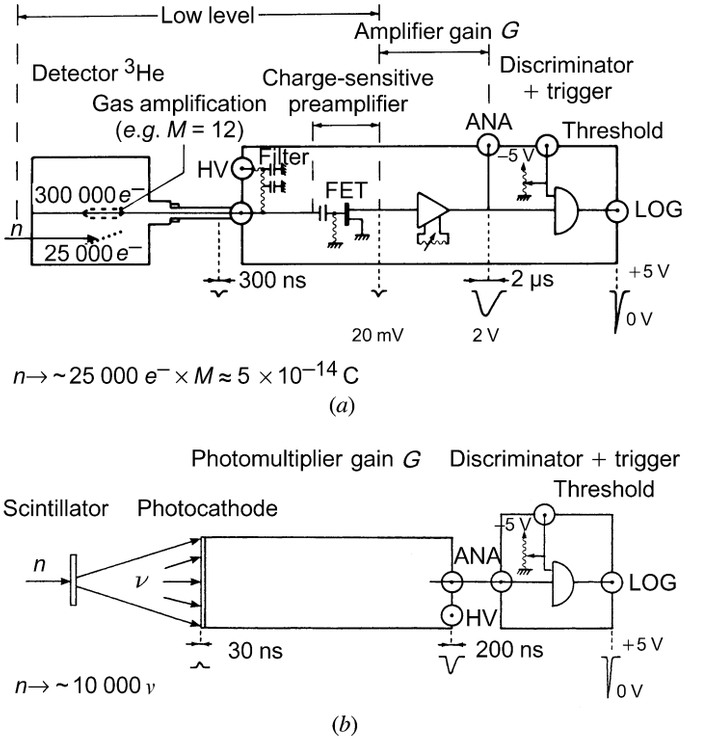

Fig. 7.3.4.1. Electronic chain following (*a*) an ^{3}He gas detector and (*b*) a scintillation detector.

references